Single-cell adhesion force mapping of a highly sticky bacterium in liquid

*Satoshi Ishii, Shogo Yoshimoto, and Katsutoshi Hori**

Department of Biomolecular Engineering, Graduate School of Engineering, Nagoya University, Furo-cho, Chikusa-ku, Nagoya, Aichi 464-8603, Japan

*Correspondence: khori@chembio.nagoya-u.ac.jp

Phone: +81-52-789-3339

Fax: +81-52-789-3218

Abstract

The highly sticky bacterium *Acinetobacter* sp. Tol 5 adheres to various material surfaces via its cell surface nanofiber protein, AtaA. This adhesiveness has only been evaluated based on the amount of cells adhering to a surface. In this study, the adhesion force mapping of a single Tol 5 cell in liquid using the quantitative imaging mode of atomic force microscopy (AFM) revealed that the strong adhesion of Tol 5 was several nanonewtons, which was outstanding compared with other adhesive bacteria. The adhesion force of a cell became stronger with the increase in AtaA molecules present on the cell surface. Many fibers of peritrichate AtaA molecules simultaneously interact with a surface, strongly attaching the cell to the surface. The adhesion force of a Tol 5 cell was drastically reduced in the presence of 1% casamino acids but not in deionized water (DW), although both liquids decrease the adhesiveness of Tol 5 cells, suggesting that DW and casamino acids inhibit the cell approaching step and the subsequent direct interaction step of AtaA with surfaces, respectively. Heterologous production of AtaA provided non-adhesive *Acinetobacter baylyi* ADP1 cells with a strong adhesion force to AFM tip surfaces of silicon and gold.

Keywords

bacterial adhesion; trimeric autotransporter adhesin; atomic force microscopy; adhesion force

1. Introduction

Bacterial adhesion causes a variety of serious problems such as infectious diseases, metal corrosion, and pathogen contamination of medical and food processing equipment [1-4]. However, bacterial adhesion can also be beneficial, for example, in bioreactors for wastewater treatment and off-gas treatment, degradation of pollutants in aqueous and soil environments, and chemical production using immobilized bacteria [5-9]. Therefore, the ability to control bacterial adhesion would be beneficial in various sectors. However, this requires a better understanding of the factors that affect bacterial adhesion.

In a typical adhesion process, bacteria attain strong adhesion in multiple steps [3]. The initial attachment of a bacterial cell to a surface is reversible and weak, and is usually described by Derjaguin−Landau−Verwey−Overbeek (DLVO) theory [10, 11]. Then, bacterial adhesion is strengthened by multiple interactions between material surfaces and surface components of bacterial cells [3, 12, 13]. In this early stage of bacterial adhesion, cell surface adhesins, which constitute cell appendages in many cases, usually interact directly with material surfaces [13]. Subsequently, cells secrete extracellular polymeric substances (EPS) during growth and finally develop tightly attached biofilms that resist detachment [3, 14]. Therefore, adhesion strength changes with time and high adhesiveness, which implies that many cells quickly attach to a surface, does not necessarily correspond to strong adhesion.

The gram-negative bacterium *Acinetobacter* sp. Tol 5 shows extremely high adhesiveness to various material surfaces from hydrophobic plastics to hydrophilic glass and metals, independent of cell growth and EPS secretion [15]. The adhesiveness of a Tol 5

cell is attributed to its peritrichate and fibrous cell appendage protein, AtaA [16-19]. AtaA is a member of the trimeric autotransporter adhesin (TAA) family and forms a long nanofiber with a length of 260 nm, which is composed of a passenger domain including the N-terminal head domain at the distal end of the fiber and the C-terminal transmembrane domain anchored to the outer membrane [16, 20]. The remarkably high adhesiveness of Tol 5 cells has been mainly evaluated by plate adherence assays using crystal violet staining, which is used to quantify the amount of bacterial cells adhering to a plate surface during incubation of a cell suspension. The adhesiveness measured by this method is a little reflective of the adhesion strength through resistance against shear stress caused by washing steps but significantly affected by attractive and repulsive forces in the initial attachment process. In addition, it is significantly affected by autoagglutination of cells because cells are stacked on a surface. Therefore, the pure adhesion strength of a bacterial cell cannot be determined by plate adherence assays. Interestingly, the adhesiveness of Tol 5 cells to any material surfaces decreases with the decrease in the ionic strength of a cell suspension and is completely lost in deionized water (DW) [21]. Also, Tol 5's cell adhesion is always drastically inhibited by casamino acids [22]. However, the underlying mechanisms that hinder the adhesion of highly sticky Tol 5 cells in these liquids remain unclear.

The purpose of the current study was to determine Tol 5's adhesion strength by the adhesion force mapping of a single cell using atomic force microscopy (AFM). Another purpose was to investigate how the adhesion force is affected in cell suspension liquids that hinder Tol 5's cell adhesion. AFM can be used to quantitatively measure the adhesion

forces of living cells and biomolecules in liquid at the sub-nanonewton level with high sensitivity by detecting the force applied to the probe upon contact with the sample [23-26]. The quantitative imaging (QI) mode is a specialized force mapping for soft and viscous samples, which combines high force sensitivity to measure adhesion with high scanning speed comparable with that of conventional tapping mode [27]. Because QI mode allows simultaneous imaging with sub-nanometer resolution and mechanical characterization with piconewton resolution in liquid without damaging delicate samples and interference by the viscosity, it has been used to study bacterial cell stiffness and adhesion [28, 29]. In this study, we performed the adhesion force mapping of a single cell of the highly sticky Tol 5 cells using QI mode in liquid.

2. Materials and Methods

2.1. Bacterial strain and growth conditions

The bacterial strains used in this study are listed in Supplementary Table S1. *Acinetobacter* sp. Tol 5, and its derivatives were grown in Luria-Bertani (LB) medium at 28°C for 8 h. *Acinetobacter baylyi* ADP1 and ADP1 (pAtaA) were grown in LB medium at 30°C for 12 h. *Yersinia enterocolitica* WA-314 was grown in LB medium at 28°C overnight, inoculated into LB medium at a 1:100 dilution, and incubated at 37°C for 8 h for *yadA* expression. *Pseudomonas fluorescens* pf0-1 and *Escherichia coli* DH5α were grown in LB medium at 37°C for 8 h, and *Bartonella henselae* was grown on Columbia agar (Oxoid Ltd., Hampshire, UK) supplemented with 5% sheep blood (Nippon Bio-Test Laboratories Ins., Saitama, Japan) in a humidified atmosphere with 5% CO_2 at 37°C. To

induce the expression of the *ataA* gene on the plasmid pAtaA, 0.5% (w/v) arabinose was added to the culture medium. The induction time was varied from 0 h to 6 h to control the amount of produced AtaA. All of the cells except *B. henselae* were harvested by centrifugation and resuspended in phosphate-buffered saline (PBS; 137 mM NaCl, 8.10 mM Na_2HPO_4, 2.68 mM KCl, and 1.47 mM KH_2PO_4, pH 7.4). The cells of *B. henselae* were collected by swabbing the agar surface with a cotton swab and suspended in PBS.

2.2. Immobilization of bacterial cells to a glass substratum

Two milliliters of 1% polyethyleneimine (Nakalai Tesque, Kyoto, Japan) solution was placed onto a glass bottom dish (FluoroDish, FD5040-100; World Precision Ins., Sarasota, FL, USA), incubated for 16 h at a room temperature (RT), and removed using a pipette. After a rinse with DW, 2 mL of 0.5% glutaraldehyde (Sigma-Aldrich, St. Louis, MO, USA) solution was placed on the surface and incubated for 2 h at RT. After rinsing with PBS, 2 mL of a bacterial cell suspension at an optical density at 660 nm of 0.1 was placed on the surface, incubated for 30 min at RT, and removed. The surface was rinsed with PBS, and 2 mL of 100 mM Tris-HCl buffer (pH 7.4) was added and incubated for 30 min at RT to inactivate unreacted glutaraldehyde. Thereafter, the solution was removed and the surface was rinsed with the same solution used for the AFM measurement described below.

2.3. Analytical methods

Force mapping was performed using NanoWizard 3 BioScience AFM system (JPK Ins., Berlin, Germany) with Advanced QI mode, which is an extensional software of QI

[27] mode at RT in PBS, PBS supplemented with 1% casamino acid technical (Becton, Dickinson and company, Franklin Lakes, NJ, USA), PBS supplemented with 1% glucose, 100 mM KCl solution, or DW. Clean silicon-probe AFM cantilevers with spring constants of 0.02-0.14 N/m (BL-AC40TS-C2; Olympus Ltd., Tokyo, Japan) or gold-coated probe cantilevers with spring constants of 0.003-0.13 N/m (HQ:CSC38/Cr-Au-B; MikroMasch, Madrid, Spain) were used. The spring constants of the cantilevers were determined using the thermal noise method. The parameters used in QI mode are the following: Z-length: 3 μm; applied force: 0.2 nN; speed: 20 μm/s.

Flow cytometry was performed as described previously [30]. AtaA on the cell surface was immune-stained with anti-$AtaA_{699\text{-}1014}$ antiserum and Alexa Fluor 488-conjugated anti-rabbit antibody (Cell Signaling Technology, Danvers, MA, USA) and detected using a flow cytometry system (FACS Canto II; Becton, Dickinson and company).

3. Results and Discussion

3. 1. Adhesion force mapping of a single cell of various bacterial strains

To compare the adhesion strength of Tol 5 with other adhesive bacteria, we performed force mapping of a single cell of Tol 5, *B. henselae* Marseille having BadA, *Y. enterocolitica* WA-314 having YadA, and *P. fluorescens* Pf0-1 having LapA as well as a non-adhesive bacterium, *E. coli* DH5α as a control. Bacterial cells were immobilized on a glass-bottom dish by a covalent bond, and thereafter the height and adhesion force between the cell surface and a silicon probe in PBS were measured in QI mode. The topographies (upper) and adhesion force maps (lower) of each single bacterial cell are shown in Figure 1.

144 The brighter colour in the topographies and in the adhesion force maps indicates the areas
145 that are higher and the areas showing a stronger adhesion force, respectively. Tol 5 showed
146 a strong adhesion force of more than several nanonewtons. BadA and YadA, like AtaA,
147 belong to the TAA family and have been reported to mediate cell adhesion to material
148 surfaces [31-33]. *P. fluorescens* pf0-1 exhibits high cell adhesion to various material
149 surfaces through LapA [34]. However, the adhesion force of these bacteria was small
150 compared with that of Tol 5, highlighting the strong adhesion of Tol 5 cells mediated by
151 AtaA. Considering the quite short contact time (< 100 ms) of a cell surface with an AFM
152 probe, a single Tol 5 cell can instantaneously attain strong adhesion to a silicon probe.
153 Recently, we showed that autoagglutination through AtaA significantly contributes to
154 biofilm formation of Tol 5 cells by triggering the formation of the biofilm [35, 36].
155 However, the current result demonstrated that a single Tol 5 cell itself has the ability to
156 very strongly adhere to a surface through the quick interaction of AtaA with the surface. It
157 is considered that the strong initial attachment capacity of Tol 5 cells using AtaA gives this
158 bacterium the property of forming a strongly attached biofilm without the secretion of EPS,
159 as shown previously [35].

160 In a previous study, bacterial cells expressing SadA, a TAA from *Salmonella enterica*,
161 have been observed using AFM [37]. However, because it was observed in air using
162 tapping mode, adverse effects on the morphology from drying were inevitable and
163 biological functions such as adhesion could not be evaluated. On the other hand, in this
164 study, we performed force mapping of Tol 5 cells expressing AtaA in liquid using QI mode.

165 To the best of our knowledge, this is the first study in which the cell morphology and
166 adhesion mediated by TAA under physiological conditions are analyzed.
167
168 **3. 2. Cell adhesion modes by AtaA**
169 To elucidate how AtaA confers the strong adhesion force to a single Tol 5 cell, we
170 prepared cells expressing the different number of AtaA molecules on the cell surface. The
171 flow cytometry of immunostained cells of Tol 5 Δ*ataA* and Tol 5 Δ*ataA* (pAtaA) cells with
172 different induction periods of *ataA* gene using anti-AtaA antiserum is shown in Figure 2A.
173 This revealed that the amount of AtaA present on the cell surface of Tol 5 Δ*ataA* (pAtaA)
174 cells increased as the induction period for the expression of the *ataA* gene on a plasmid
175 with arabinose was extended. Subsequently, they were subjected to force mapping on a
176 single cell surface. Tol 5 Δ*ataA* and 0-h induced (uninduced) Tol 5 Δ*ataA* (pAtaA) cells
177 showed little adhesion force and the adhesion force of Tol 5 Δ*ataA* (pAtaA) cells became
178 stronger as the induction period increased and the amount of AtaA present on the cell
179 surface increased (Fig. 2B). The 6-h induced Tol 5 Δ*ataA* (pAtaA) cells accumulated more
180 AtaA molecules on their cell surface and showed stronger cell adhesion than the Tol 5 wild
181 type (WT) cells.
182 Biaxial graphs of height and adhesion force obtained from cross sections of single cell
183 AFM images of 2-h induced Tol 5 Δ*ataA* (pAtaA) and Tol 5 Δ*ataA* are shown in Figures 3
184 and S1, respectively. Even in liquid, peritrichate AtaA fibers covering the cell surface could
185 be visualized at the margin of the cell in a high-resolution image (Fig. 3A) and they were
186 not observed in Tol 5 Δ*ataA* (Fig. S1A). Peaks of adhesion force of 1 to 2 nN were recorded

187 along the cross-sectional lines on a Tol 5 Δ*ataA* (pAtaA) cell (Fig 3B and C), whereas a Tol
188 5 Δ*ataA* cell showed little interaction with the AFM probe (Fig. S1B and C). On both the
189 short and long axes of the Tol 5 Δ*ataA* (pAtaA) cell, stronger adhesions tended to be
190 recorded at the margin of the cell where the AtaA fibers laterally extend than at the upper
191 side of the cell (Fig. 3B and C). This tendency was observed at various cross sections on
192 this mutant cell (Fig. S2). This is probably because the AFM probe can make contact with
193 more AtaA fibers at the margin of a cell than the upper side, as shown in Figure S3. Thus,
194 many fibers of Tol 5 peritrichate AtaA molecules simultaneously interact with a surface,
195 strongly attaching the cell to the surface.
196
197 **3. 3. Measurement of adhesion strength of a single Tol 5 cell under conditions of**
198 **adhesion inhibition**
199 We investigated whether the adhesion strength of Tol 5 is lost or reduced in a casamino
200 acids solution and DW, in which the adhesion of Tol 5 cells is known to be hindered. Force
201 mapping using QI mode confirmed that the adhesion force of a Tol 5 cell drastically
202 reduced in the presence of 1% casamino acids but not in the presence of 1% glucose (Fig.
203 4A). The adhesion strength of Tol 5 cells lost in 1% casamino acids solution could be
204 recovered by replacing the solution with fresh PBS. This suggested that casamino acids
205 inhibit the interaction between AtaA and the silicon AFM probe without denaturing AtaA,
206 which was consistent with previous results [22]. Surprisingly, in contrast to casamino acids
207 solution, the adhesion force measured in DW was almost the same as that measured in PBS
208 and 100 mM KCl (Fig. 4B), indicating that the salt concentration did not affect the

adhesion strength of Tol 5. Note that the topography of the cells in DW was the same as that observed in PBS and 100 mM KCl (Fig. 4), confirming that no adverse effects such as cell lysis were caused by osmotic stress.

Although both the presence of casamino acids and the low ionic strength conditions are critical for the adhesion of Tol 5 cells, their effects on the adhesion force are quite different, suggesting that the mechanisms that inhibit cell adhesion in these media are different. Before adhering to a surface, a cell must approach the surface to a position from which AtaA can make contact with it [35]. According to the DLVO theory, during this approaching process, a bacterial cell undergoes both attractive and repulsive forces from a surface, and their summation directly affects cell adhesion. It has been shown that autoagglutination of Tol 5 cells follows the DLVO theory [35], and it can be considered that the interaction between the cell and the surface also follows this theory. At lower ionic strength, the repulsive force is stronger and both cell adhesion and autoagglutination are hindered [8]. AtaA fibers cannot make contact with a surface for adhesion or with each other for autoagglutination because of the long distance between a Tol 5 cell body and its interaction targets (a surface or another cell). Therefore, the adhesiveness of Tol 5 cells is lost in DW. On the other hand, in QI mode of AFM, an AFM probe was forced to make contact with a Tol 5 cell before the adhesion force measurement. Therefore, adhesion force corresponds to the force required for the detachment, that is, the resistance force for detaching an AFM probe from a cell. This process is not affected by the ionic strength. Therefore, once AtaA comes into contact with a surface even in DW, it exhibits a strong adhesion force and shows high resistance to peeling.

In contrast, it is considered that casamino acids directly inhibit the interaction between an AtaA molecule and a material surface, resulting in the reduction of the adhesion force. For example, component molecules in casamino acids may adsorb onto the AtaA molecules, blocking contact between AtaA fibers and the surface. Therefore, AFM unexpectedly revealed that there are two different steps for inhibition of the initial attachment of a bacterial cell to a surface, that is, the cell approaching step and subsequent direct interaction step between adhesins and surfaces. DW and casamino acids inhibit the cell adhesion in the first step and the second step, respectively. AFM gives us a lot of additional information about cell adhesion that cannot be obtained with a plate adherence assay.

3. 4. Evaluation of the adhesion strength of AtaA in another bacterium using different probe materials

The adhesiveness of AtaA can be conferred to other non-adhesive bacteria by heterologous expression of the *ataA* gene [16, 21, 38, 39]. We have developed a new cell immobilization method using AtaA and have demonstrated its effectiveness in microbial green production processes [38-41]. Furthermore, cells immobilized with AtaA can be detached using liquids that inhibit cell adhesion, that is, washing with DW or the addition of casamino acids, and the detached cells can be re-immobilized in a salt medium or in a buffer solution [21, 22]. As shown in the current study, this implies that AtaA-mediating cell adhesion is strong but reversible and, therefore, attached cells can be detached if the cells undergo a shear stress that is stronger than the adhesion force. In bioreactor operation,

it is important for immobilized cells to exhibit an adhesion strength that is sufficient for stable immobilization against the shear stress generated by liquid flows in bioreactors. Another important feature of the cell adhesion mediated by AtaA is its nonspecificity, which enables cells to immobilize on various material surfaces. Therefore, we performed adhesion force mapping of cell surfaces of *A. baylyi* ADP1 and its *ataA*-expressing strain *A. baylyi* ADP1 (pAtaA) [42] using probes that have a bare silicon tip and a fully gold-coated one. ADP1 (pAtaA) cells showed adhesion forces as strong as Tol 5 cells not only to the silicon tip but also to the gold-coated tip (Fig. 5), whereas the ADP1 WT showed small adhesion force. Thus, it was demonstrated that the heterologous production of AtaA can provide originally non-adhesive bacteria with adhesion strength that is strong for stable immobilization to various materials. Because the adhesion force is controllable by the expression level of the *ataA* gene (Fig. 2), a desirable adhesion strength for reversible immobilization can be provided to the bacterial cells.

4. Conclusions

In this study, we performed adhesion force mapping of a single cell of *Acinetobacter* sp. Tol 5 using QI mode of AFM in liquid. Tol 5 cells showed a much stronger adhesion force than those of other adhesive bacteria including species that have a TAA other than AtaA in PBS. The adhesion force of a cell became stronger with the increase in AtaA molecules present on the cell surface. Peritrichate AtaA fibers extending laterally were visualized in a high-resolution image in liquid at the margin of the cell, in which stronger adhesions tended to be recorded than at the top side of the cell by cross sectioning of the

cell force maps. Peaks of adhesion force of 1 to 2 nN were recorded along the cross-sectional lines of Tol 5 cells expressing AtaA. Many fibers of peritrichate AtaA molecules interact simultaneously to a surface, strongly attaching the cell to the surface. The adhesion force of a Tol 5 cell was drastically reduced in the presence of 1% casamino acids but not in DW, although both liquids decrease the adhesiveness of Tol 5 cells, as quantified by plate adherence assays. The QI mode of AFM, in which a probe is forced to make contact with a cell surface, revealed that DW inhibits the first cell-approaching step and casamino acids inhibit the subsequent direct interaction step between adhesins and surfaces. AFM gave us different insights on cell adhesion from the plate adherence assay. *A. baylyi* ADP1 expressing the *ataA* gene showed a strong adhesion force to both silicon- and gold-coated AFM probe tips, demonstrating that the heterologous production of AtaA can provide originally non-adhesive bacteria with strong adhesion capacity for stable immobilization to various materials.

CRediT authorship contribution statement

Satoshi Ishii: Investigation, Writing - Original Draft. **Shogo Yoshimoto:** Writing - Original Draft, Funding acquisition. **Katsutoshi Hori:** Conceptualization, Writing - Review & Editing, Supervision, Funding acquisition.

Declaration of Competing Interest

The authors declare no conflict of interest.

Acknowledgments

We thank Volkhard A. J. Kempf and Stephan Göttig from the Goethe University for providing *Bartonella henselae* Marseille. We also thank Hideaki Nojiri from the University of Tokyo for providing *Pseudomonas fluorescens* Pf0-1. This work was supported by the Japan Society for the Promotion of Science (JSPS) KAKENHI (Grant Numbers JP17H01345, JP18K14062).

References

1. Beech, W.B. and Sunner, J., *Biocorrosion: towards understanding interactions between biofilms and metals.* Current Opinion in Biotechnology, 2004. **15**(3): 181-186.
2. Harro, J.M., Peters, B.M., O'May, G.A., Archer, N., Kerns, P., Prabhakara, R., and Shirtliff, M.E., *Vaccine development in Staphylococcus aureus: taking the biofilm phenotype into consideration.* FEMS Immunology & Medical Microbiology, 2010. **59**(3): 306-323.
3. Donlan, R.M., *Biofilm formation: A clinically relevant microbiological process.* Clinical Infectious Diseases, 2001. **33**(8): 1387-1392.
4. Scharff, R.L., *Economic burden from health losses due to foodborne illness in the United States.* Journal of Food Protection, 2012. **75**(1): 123-131.
5. Bouwer, E.J. and Zehnder, A.J.B., *Bioremediation of organic-compounds - putting microbial-metabolism to work.* Trends in Biotechnology, 1993. **11**(8): 360-367.
6. Macdonald, J.A. and Rittmann, B.E., *Performance standards for in-situ bioremediation.* Environmental Science & Technology, 1993. **27**(10): 1974-1979.
7. Marjaka, I.W., Miyanaga, K., Hori, K., Tanji, Y., and Unno, H., *Augmentation of self-purification capacity of sewer pipe by immobilizing microbes on the pipe surface.* Biochemical Engineering Journal, 2003. **15**(1): 69-75.
8. Hori, K. and Matsumoto, S., *Bacterial adhesion: From mechanism to control.* Biochemical Engineering Journal, 2010. **48**(3): 424-434.
9. Qureshi, N., Annous, B.A., Ezeji, T.C., Karcher, P., and Maddox, I.S., *Biofilm reactors for industrial bioconversion processes: employing potential of enhanced reaction rates.* Microbial Cell Factories, 2005. **4**: 24.
10. Meinders, J.M., vanderMei, H.C., and Busscher, H.J., *Deposition efficiency and reversibility of bacterial adhesion under flow.* Journal of Colloid and Interface Science, 1995. **176**(2): 329-341.
11. Marshall, K.C., Stout, R., and Mitchell, R., *Mechanism of the initial events in the sorption of marine bacteria to surfaces.* Journal of General Microbiology, 1971. **68**: 337-348.
12. Palmer, J., Flint, S., and Brooks, J., *Bacterial cell attachment, the beginning of a biofilm.* Journal of Industrial Microbiology & Biotechnology, 2007. **34**(9): 577-588.
13. Kline, K.A., Falker, S., Dahlberg, S., Normark, S., and Henriques-Normark, B., *Bacterial adhesins in host-microbe interactions.* Cell Host & Microbe, 2009. **5**(6): 580-592.

14. Simoes, M., Simoes, L.C., and Vieira, M.J., *A review of current and emergent biofilm control strategies.* LWT-Food Science and Technology, 2010. **43**(4): 573-583.
15. Ishikawa, M., Shigemori, K., Suzuki, A., and Hori, K., *Evaluation of adhesiveness of Acinetobacter sp. Tol 5 to abiotic surfaces.* Journal of Bioscience and Bioengineering, 2012. **113**(6): 719-725.
16. Ishikawa, M., Nakatani, H., and Hori, K., *AtaA, a new member of the trimeric autotransporter adhesins from Acinetobacter sp. Tol 5 mediating high adhesiveness to various abiotic surfaces.* PLoS One, 2012. **7**(11): e48830.
17. Hori, K., Ishikawa, M., Yamada, M., Higuchi, A., Ishikawa, Y., and Ebi, H., *Production of peritrichate bacterionanofibers and their proteinaceous components by Acinetobacter sp. Tol 5 cells affected by growth substrates.* Journal of Bioscience and Bioengineering, 2011. **111**(1): 31-36.
18. Ishii, S., Koki, J., Unno, H., and Hori, K., *Two morphological types of cell appendages on a strongly adhesive bacterium, Acinetobacter sp. strain Tol 5.* Applied and Environmental Microbiology, 2004. **70**(8): 5026-5029.
19. Ishii, S., Miyata, S., Hotta, Y., Yamamoto, K., Unno, H., and Hori, K., *Formation of filamentous appendages by Acinetobacter sp. Tol 5 for adhering to solid surfaces.* Journal of Bioscience and Bioengineering, 2008. **105**(1): 20-25.
20. Koiwai, K., Hartmann, M.D., Linke, D., Lupas, A.N., and Hori, K., *Structural basis for toughness and flexibility in the C-terminal passenger domain of an Acinetobacter trimeric autotransporter adhesin.* Journal of Biological Chemistry, 2016. **291**(8): 3705-3724.
21. Yoshimoto, S., Ohara, Y., Nakatani, H., and Hori, K., *Reversible bacterial immobilization based on the salt-dependent adhesion of the bacterionanofiber protein AtaA.* Microbial Cell Factories, 2017. **16**(1): 123.
22. Ohara, Y., Yoshimoto, S., and Hori, K., *Control of AtaA-mediated bacterial immobilization by casein hydrolysates.* Journal of Bioscience and Bioengineering, 2019. **128**(5): 544-550.
23. Elbourne, A., Chapman, J., Gelmi, A., Cozzolino, D., Crawford, R.J., and Truong, V.K., *Bacterial-nanostructure interactions: The role of cell elasticity and adhesion forces.* Journal of Colloid and Interface Science, 2019. **546**: 192-210.
24. Hansma, H.G., Kim, K.J., Laney, D.E., Garcia, R.A., Argaman, M., Allen, M.J., and Parsons, S.M., *Properties of biomolecules measured from atomic force microscope images: A review.* Journal of Structural Biology, 1997. **119**(2): 99-108.

25. Krieg, M., Flaschner, G., Alsteens, D., Gaub, B.M., Roos, W.H., Wuite, G.J.L., Gaub, H.E., Gerber, C., Dufrene, Y.F., and Muller, D.J., *Atomic force microscopy-based mechanobiology.* Nature Reviews Physics, 2019. **1**(1): 41-57.

26. Harimawan, A., Rajasekar, A., and Ting, Y.P., *Bacteria attachment to surfaces - AFM force spectroscopy and physicochemical analyses.* Journal of Colloid and Interface Science, 2011. **364**(1): 213-218.

27. Chopinet, L., Formosa, C., Rols, M.P., Duval, R.E., and Dague, E., *Imaging living cells surface and quantifying its properties at high resolution using AFM in QI (TM) mode.* Micron, 2013. **48**: 26-33.

28. Mathelie-Guinlet, M., Asmar, A.T., Collet, J.F., and Dufrene, Y.F., *Lipoprotein Lpp regulates the mechanical properties of the E. coli cell envelope.* Nature Communications, 2020. **11**: 1789.

29. Casdorff, K., Keplinger, T., and Burgert, I., *Nano-mechanical characterization of the wood cell wall by AFM studies: comparison between AC- and QI (TM) mode.* Plant Methods, 2017. **13**: 60.

30. Aoki, S., Yoshimoto, S., Ishikawa, M., Linke, D., Lupas, A., and Hori, K., *Native display of a huge homotrimeric protein fiber on the cell surface after precise domain deletion.* Journal of Bioscience and Bioengineering, 2020. **129**(4): 412-417.

31. Riess, T., Andersson, S.G.E., Lupas, A., Schaller, M., Schafer, A., Kyme, P., Martin, J., Walzlein, J.H., Ehehalt, U., Lindroos, H., Schirle, M., Nordheim, A., Autenrieth, I.B., and Kempf, V.A.J., *Bartonella adhesin A mediates a proangiogenic host cell response.* Journal of Experimental Medicine, 2004. **200**(10): 1267-1278.

32. El Tahir, Y. and Skurnik, M., *YadA, the multifaceted Yersinia adhesin.* International Journal of Medical Microbiology, 2001. **291**(3): 209-218.

33. Muller, N.F., Kaiser, P.O., Linke, D., Schwarz, H., Riess, T., Schafer, A., Eble, J.A., and Kempf, V.A.J., *Trimeric autotransporter adhesin-dependent adherence of Bartonella henselae, Bartonella quintana, and Yersinia enterocolitica to matrix components and endothelial cells under static and dynamic flow conditions.* Infection and Immunity, 2011. **79**(7): 2544-2553.

34. Compeau, G., Alachi, B.J., Platsouka, E., and Levy, S.B., *Survival of rifampin-resistant mutants of Pseudomonas-fluorescens and Pseudomonas-putida in soil systems.* Applied and Environmental Microbiology, 1988. **54**(10): 2432-2438.

35. Furuichi, Y., Yoshimoto, S., Inaba, T., Nomura, N., and Hori, K., *Process description of an unconventional biofilm formation by bacterial cells autoagglutinating through sticky, long, and peritrichate nanofibers.* Environmental Science & Technology, 2020. **54**(4): 2520-2529.
36. Furuichi, Y., Iwasaki, K., and Hori, K., *Cell behavior of the highly sticky bacterium Acinetobacter sp. Tol 5 during adhesion in laminar flows.* Scientific Reports, 2018. **8**: 8285.
37. Hansmeier, N., Miskiewicz, K., Elpers, L., Liss, V., Hensel, M., and Sterzenbach, T., *Functional expression of the entire adhesiome of Salmonella enterica serotype Typhimurium.* Scientific Reports, 2017. **7**(1): 10326.
38. Ishikawa, M., Shigemori, K., and Hori, K., *Application of the adhesive bacterionanofiber AtaA to a novel microbial immobilization method for the production of indigo as a model chemical.* Biotechnology and Bioengineering, 2014. **111**(1): 16-24.
39. Nakatani, H., Ding, N., Ohara, Y., and Hori, K., *Immobilization of Enterobacter aerogenes by a trimeric autotransporter adhesin, AtaA, and its application to biohydrogen production.* Catalysts, 2018. **8**(4): 159.
40. Noba, K., Ishikawa, M., Uyeda, A., Watanabe, T., Hohsaka, T., Yoshimoto, S., Matsuura, T., and Hori, K., *Bottom-up creation of an artificial cell covered with the adhesive bacterionanofiber protein AtaA.* Journal of the American Chemical Society, 2019. **141**(48): 19058-19066.
41. Usami, A., Ishikawa, M., and Hori, K., *Gas-phase bioproduction of a high-value-added monoterpenoid (E)-geranic acid by metabolically engineered Acinetobacter sp. Tol 5.* Green Chemistry, 2020. **22**(4): 1258-1268.
42. Hori, K., Ohara, Y., Ishikawa, M., and Nakatani, H., *Effectiveness of direct immobilization of bacterial cells onto material surfaces using the bacterionanofiber protein AtaA.* Applied Microbiology and Biotechnology, 2015. **99**(12): 5025-5032.

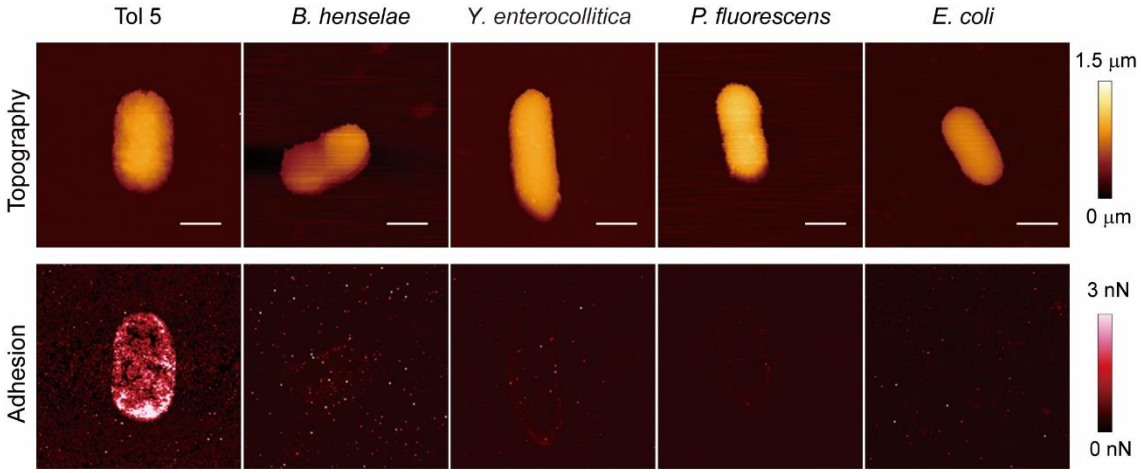

417

418 Fig. 1. Adhesion force mapping of bacterial cells. Topographies (upper) and adhesion force

419 maps (lower) of *Acinetobacter* sp. Tol 5, *Bartonella henselae* Marseille, *Yersinia*

420 *enterocolitica* WA-314, *Pseudomonas fluorescens* pf0-1, and *Escherichia coli* DH5α. Maps

421 were obtained in PBS by QI mode (128 px^2, *x*-range: 5 µm). Scale bars: 1 µm.

422

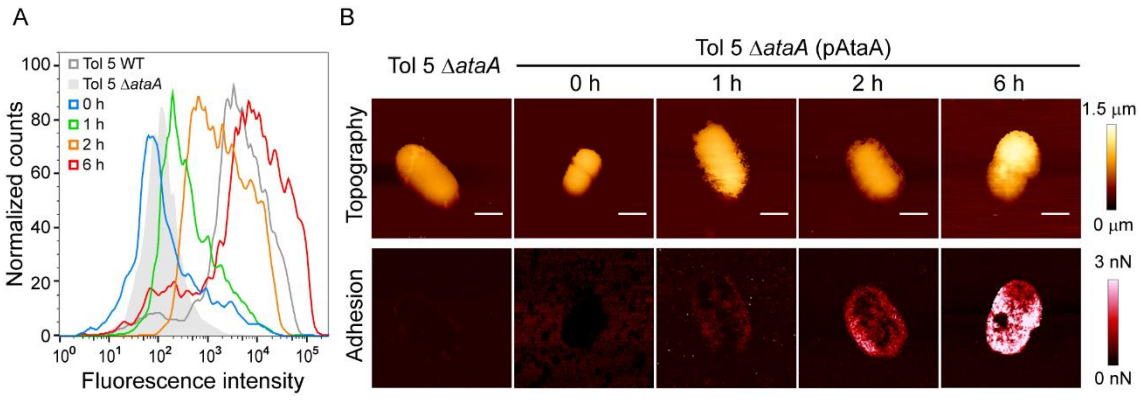

Fig. 2. Effect of the number of AtaA fibers displayed on the cells surface on the adhesion force of Tol 5's cells. (A) Flow cytometry of Tol 5, Tol 5 Δ*ataA,* and Tol 5 Δ*ataA* (pAtaA) cells with different induction periods for *ataA* gene expression (0, 1, 2, and 6 h) using anti-AtaA antiserum. (B) Adhesion force mapping of Tol 5 Δ*ataA* and Tol 5 Δ*ataA* (pAtaA) with different induction periods for *ataA* gene expression. Topographies (upper) and adhesion force maps (lower) were obtained in PBS by QI mode (128 px^2, x-range: 5 µm). Scale bars: 1 µm.

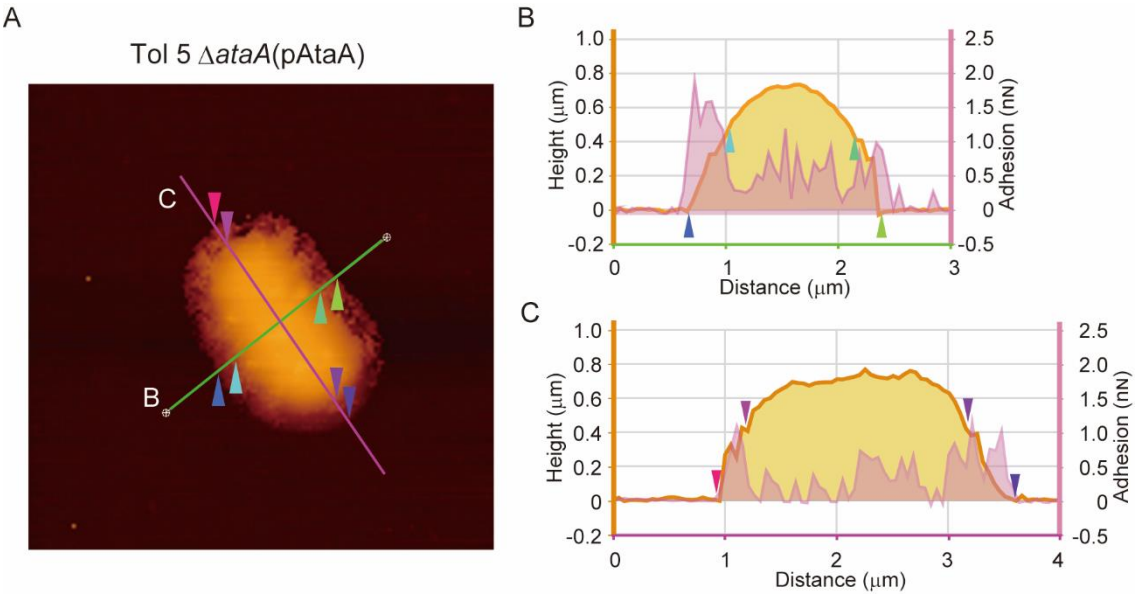

Fig. 3. Cross-section analysis of cell adhesion via AtaA. (A) Topography of a Tol 5 Δ*ataA* (pAtaA) cell with an induction period of 2 h for the *ataA* gene expression obtained by QI mode in liquid. The green and magenta lines with arrowheads indicate cross-section positions. (B) & (C) Height and adhesion forces recorded on the cell along the green line (B) and the magenta line (C) shown in (A). The positions marked by colored triangles shown in (A) correspond to those with the same color shown in (B) & (C).

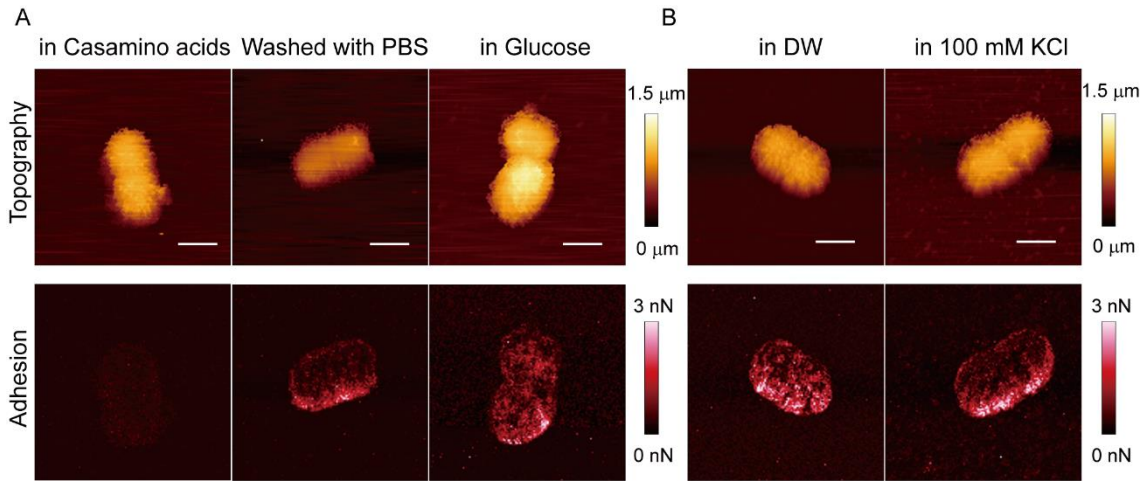

Fig. 4. Adhesion force mapping of Tol 5 cells in casamino acids solution and deionized water (DW). Topographies (upper) and adhesion force maps (lower) of Tol 5 cells in (A) 1% casamino acids solution, PBS replaced from 1% casamino acids solution, 1% glucose solution, and in (B) DW and 100 mM KCl solution. Topographies and adhesion force maps were obtained by QI mode (128 px^2, x-range: 5 μm). Scale bars: 1 μm.

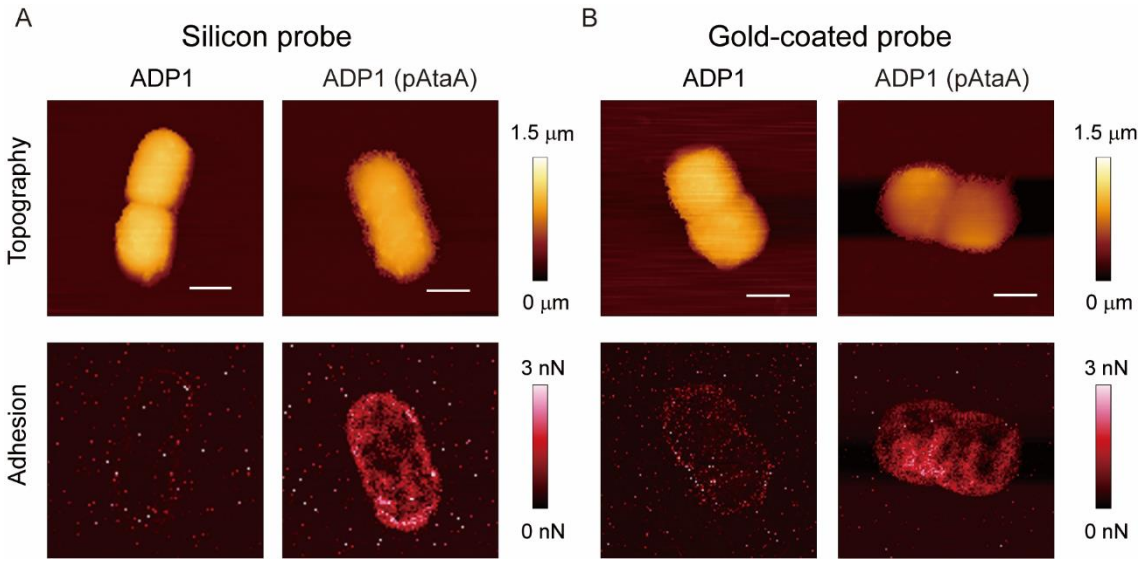

Fig. 5. Adhesion force mapping of *Acinetobacter baylyi* ADP1 and ADP1 (pAtaA) cells. Topographies (upper) and adhesion force maps (lower) were obtained in PBS by QI mode (128 px^2, x-range: 5 µm) with (A) a silicon probe and (B) a gold-coated probe. Scale bars: 1 µm.

Supporting Information

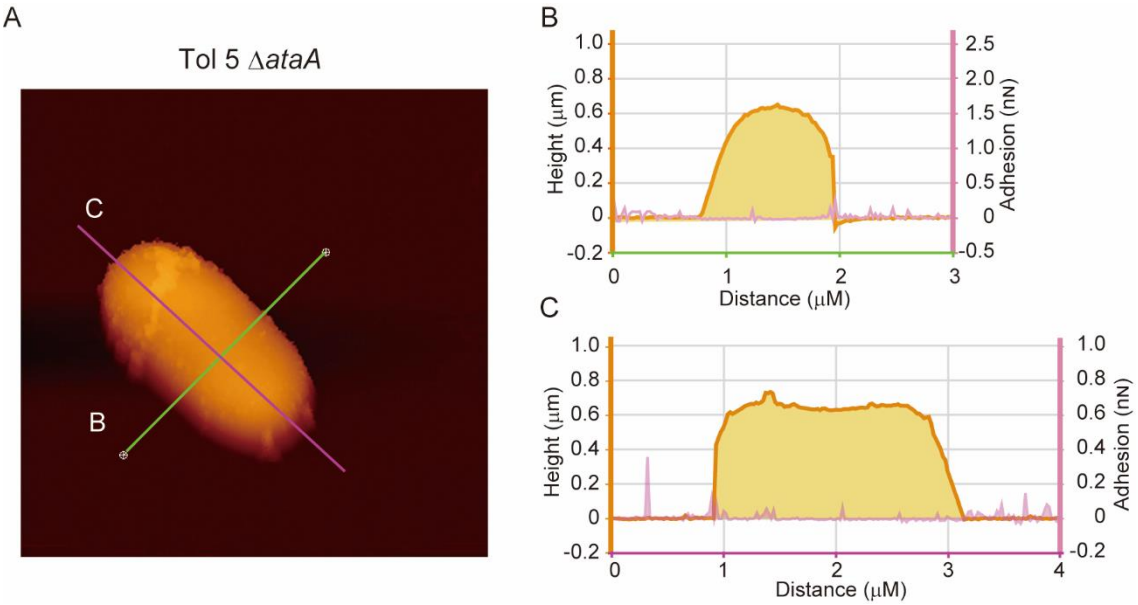

Fig. S1. Cross-section analysis of Tol 5 Δ*ataA*. (A) Topography obtained by QI mode in liquid. The green and magenta lines indicate the cross-section positions. (B) & (C) Height and adhesion forces recorded on a Tol 5 Δ*ataA* cell along the green line (B) and the magenta line (C) shown in (A).

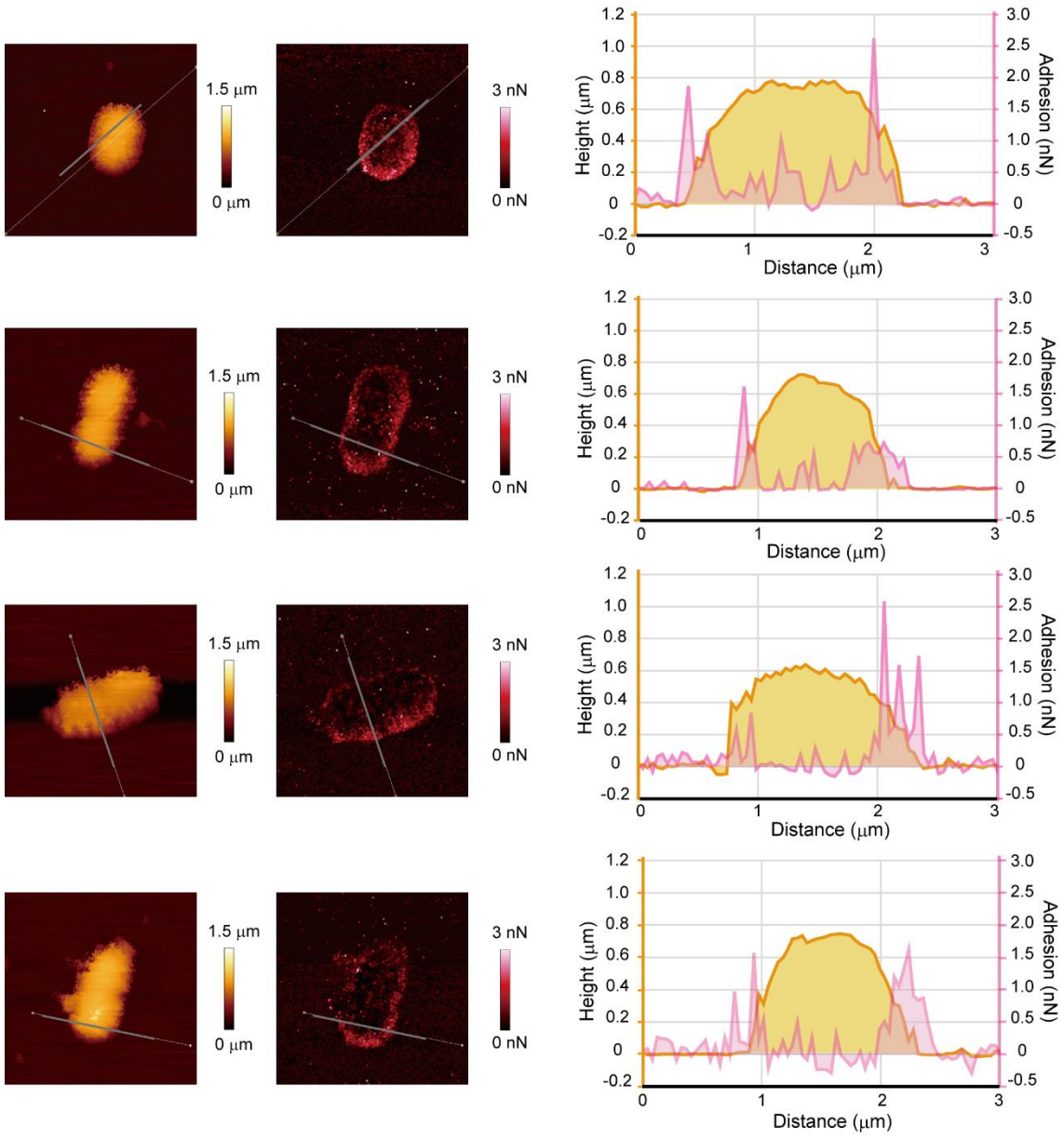

462

463 Fig. S2. Cross-section analyses of Tol 5 Δ*ataA* (pAtaA) cells with an induction period of 2

464 h for *ataA* gene expression obtained by QI mode (128 px^2, x-range: 5 µm) in PBS.

465 Topographies (left), adhesion force maps (center), and height and adhesion force along the

466 gray line shown in the topographies.

467

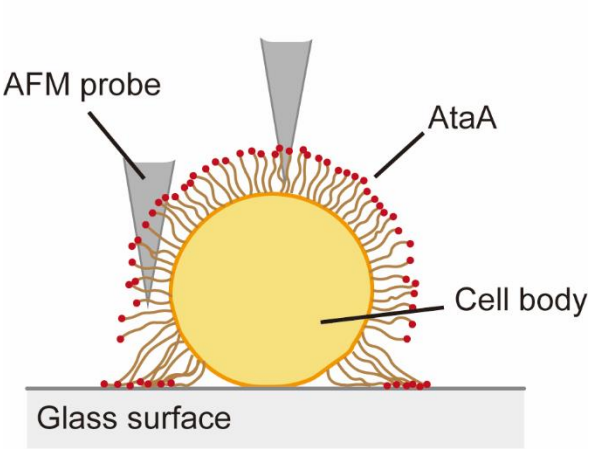

468

469 Fig. S3. Schematic illustration for force mapping of a Tol 5 cell by QI mode.

470

471

472 Table S1. Bacterial strains used in this study.

Strain	Description	Reference
Acinetobacter sp. Tol 5	Wild type strain, expressing *ataA*	[16]
Acinetobacter sp. Tol 5 Δ*ataA*	*Acinetobacter* sp. Tol 5 4140, Unmarked Δ*ataA* mutant of Tol 5, *ataA*$^-$	[38]
Acinetobacter sp. Tol 5 Δ*ataA* (pAtaA)	Previously generated *ataA*-complementary strain, harboring plasmid pAtaA, expressing *ataA* during L-arabinose induction	[38]
Bartonella henselae	*B. henselae* Marseille, Patient isolate, expressing *badA*	[31]
Yersinia enterocolitica	*Y. enterocolitica* WA-314 serotype O:8, harboring plasmid pYV, expressing *yadA*	[32]
Pseudomonas fluorescens	*P. fluorescens* Pf0-1, expressing *lapA*	[34]
Escherichia coli	*E. coli* DH5α	Takara
Acinetobacter baylyi ADP1	Wild type strain	ATCC 33305
Acinetobacter baylyi ADP1 (pAtaA)	Previously generated *ataA*-expressing strains, harboring plasmid pAtaA, expressing *ataA* during L-arabinose induction	[42]

473